Engineering Fracture Mechanics 210 (2019) 429–443

Contents lists available at ScienceDirect

Engineering Fracture Mechanics

journal homepage: www.elsevier.com/locate/engfracmech

Structural monitoring and assessment of an ancient masonry tower

Stefano Invernizzi[a,*], Giuseppe Lacidogna[a], Natalia E. Lozano-Ramírez[b], Alberto Carpinteri[a]

[a] Department of Structural, Geotechnical and Building Engineering, Politecnico di Torino, Corso Duca degli Abruzzi 24, Torino 10129, Italy
[b] Civil Engineering Department, Pontificia Universidad Javeriana, Carrera 7 No. 40 – 62 Edif. No. 42, Bogotá, DC, Colombia

ARTICLE INFO

Keywords:
Acoustic emissions
Finite element analysis
Fracture mechanics
Damage
Masonry

ABSTRACT

The Asinelli Tower in Bologna is taken as a case study to define a general methodology for the analysis of historical masonry towers. The difficulties that are typically encountered in building finite element models of increasing complexity are addressed, proposing a general procedure. A formulation accounting for masonry anisotropy due to existing damage and cracking is presented, which is more effective in describing the dynamic behavior of the tower, compared with results available in the literature. In addition, acoustic emission monitoring results are presented and compared to the numerical simulations. The structural assessment of the tower is carried out with respect to different actions like seismicity, wind and urban traffic.

1. Introduction

The increasing computational power of nowadays workstations and personal computer allows for the finite element simulation of large structural models, with increasing number of elements and accounting for mechanical and geometrical nonlinearities. In the case of existing structures, this is made possible also thanks to advanced survey techniques, like terrestrial photogrammetry and laser scanning, and several moderately destructive and non-destructive techniques, such as dynamic identification and acoustic emission monitoring. As a consequence, especially in the case of exceptional and singular structures, it is not always obvious which is the optimal level of discretization to be adopted when preparing the structural model. In the present study, the typology of existing ancient masonry towers is considered.

The Asinelli Tower in Bologna (Italy) is taken as a case study to investigate a general approach to the finite element modeling of such kind of structures. The tower is quite well documented, since it has been subjected to several experimental and numerical investigations by different authors, whose results are available in the literature [1–3].

Three models, with increasing details, are considered. The first accounts only for the principal geometrical features, nevertheless including the tower deviation from verticality. The second model accounts also for the structure of the ‘a sacco’ three-leaf masonry wall, while the third and more complex model includes also the exact geometry representation of the tower, accounting for the presence of the surrounding arcade, the presence of openings, the presence of steel-tie reinforcements put in place in the past, as well as accurate modeling of the pile foundation. The numerical results are compared to experimental results obtained from dynamic identification, as well as with other numerical results from other authors. It is shown that it is not possible to obtain a proper value of the torsional modal frequency, if damage-induced cracking and anisotropy of the masonry is not considered explicitly. The pushover analysis suggests that for the present tower the structural reduction factor of the elastic spectrum should be lower than what is suggested by the National standards.

* Corresponding author.
E-mail address: stefano.invernizzi@polito.it (S. Invernizzi).

https://doi.org/10.1016/j.engfracmech.2018.05.011
Received 13 March 2018; Received in revised form 7 May 2018; Accepted 7 May 2018
Available online 23 May 2018

Nomenclature

FEM	finite element modeling
GPR	Ground Penetrating Radar
MDOF	Multiple Degree of Freedom
MPA	modal pushover analysis
SDOF	Single Degree of Freedom
TLS	Terrestrial Laser-Scanning
d	damage parameter
D^{I}_{secant}	secant stiffness parameter I
D^{II}_{secant}	secant stiffness parameter II
ε^{cr}	individual crack strain
ε_i^{cr}	crack i strain
E	Young's modulus
E_H, E_1, E_2	Young's modulus in the horizontal direction [N/m^2]
E_V, E_3	Young's modulus in the vertical direction [N/m^2]
G	shear modulus
G_{13}, G_{23}	shear modulus normal to the E_2 and E_1 direction respectively [N/m^2]
G_{12}	shear modulus normal to the E_3 direction [N/m^2]
$[H]^{-1}$	matrix of elastic coefficients
i	crack index
N	transformation matrix
$n-t$	coordinate system
σ_i	crack i stress [N/m^2]
ε	total strain
ε^{e}	elastic strain
ε^{cr}	crack strain
μ	reduction factor of E
β	reduction factor of G
ν_{ij}	Poisson coefficient

Finally, the numerical results are compared to acoustic emission monitoring data of the Asinelli Tower, recorded by the authors previously [4]. The acoustic emissions recorded during the monitoring period can be compared, in a statistical fashion, with the recorded intensity of wind thrust and urban traffic. On the other hand, seismic events recorded during the monitoring period in the nearby region of the tower, can be compared with prior and subsequent acoustic emission activity recorded in the tower. The comparison allows for a structural assessment of the tower discriminating among the different considered actions.

1.1. Case study

The Asinelli Tower is located in the old town of the city of Bologna, Italy. It is the tallest and oldest masonry tower built in Bologna, and the tallest leaning tower in Italy. It stands as the symbol of the city, together with its adjoining tower: the Garisenda [3]. Furthermore, the medieval construction remains as one of the most important models of Italian cultural heritage and masonry buildings in the world. The approximately 97 m high tower has a square cross-section which sides taper along its height, measuring from 8 m at the bottom to 6.5 m at the top. The tower weights approximately 7300 metric tons.

The structure of the tower can be divided in four main parts in height depending on the characteristics of the cross-section and differences in masonry material, from the bottom to the top, as shown in Fig. 1: a selenite-stone-block and rubble masonry wall structure of about 3 m high (segment A), followed by a 31 m brick and rubble masonry wall (segment B), a 25 m brick and rubble masonry wall of shorter thickness (segment C) and a 38 m solid-brick-masonry wall cross-section holding the belfry at the top (segment D). The first 10 m of the tower are surrounded by a masonry portico [3,4].

The tower has been reinforced over the last centuries through a series of steel cables and chains. These elements are positioned in a horizontal direction surrounding the cross-section of the tower and also positioned in such a way that compression forces induced by the steel chains would strengthen the construction.

The tower's foundation is composed of a solid-stone masonry base just below the ground level, followed by a 4.8 m stone-pebble-and-lime conglomerate layer with high levels of compaction, ending with a series of underpinning wood piles in a non-optimal conservation state [5,6].

1.2. Recent research on the Asinelli tower

The Asinelli tower in Bologna, Italy has been the objective of a series of innovative studies on the geometry and material properties in the last decades. In 1998, the first phase of an intervention program started, including in situ and laboratory analyses and a monitoring and control system for both the Garisenda and the Asinelli towers [6]. Subsequently, Riva et al. [7] presented a one-dimensional finite element beam model, idealizing the tower with 21 linear elastic segments with different cross section connected by nonlinear joints in correspondence of the most relevant discontinuities in the actual tower. The foundation was modeled as a rigid block with six springs and dashpots to account for soil-structure interaction. In this way, modal and seismic analyses of the tower were performed.

The new technologies allowed researches to create digital models of the towers that translate all the information found and performed a series of simulations and calculations in order to plan future consolidation and reinforcement procedures. These studies allowed the constant control of fatigue of the walls and materials related to dead weight, wind, seismic and traffic vibration loads [6].

Between 2010 and 2011, a metallographic study is carried out to determine the chemical and physical characterization of the metallic belt and chain elements from 1706 and 1913, basically on exact replicas to avoid an invasive approach [6]. However, a sample was taken in site from an accessory element from which some specimens were extracted and subjected to laboratory tests.

In 2012, TECNO IN S.p.A. and the Italian National Institute of Geophysics and Volcanology (INGV) were in charge of the monitoring of Asinelli and Garisenda towers [8], to control their behavior over time through a series of seismic stations with

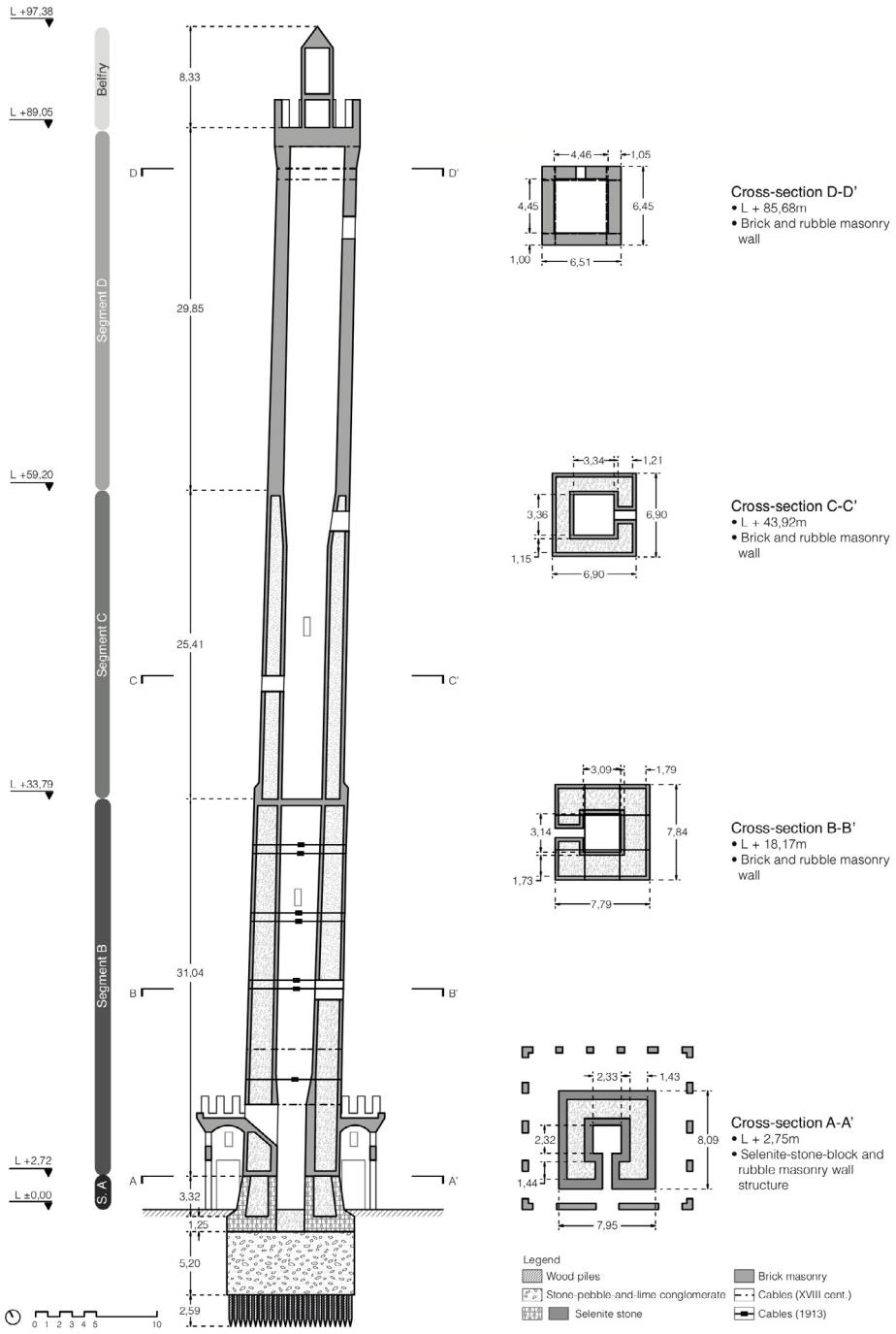

Fig. 1. Asinelli tower: vertical south section and cross-sections of the structure.

seismometric three-axial sensors. This study made possible to obtain the frequencies associated with the vibration modes of both towers.

More recently, the Acoustic Emission (AE) technique was used for the assessment of the tower's structural stability [4,9,10].

In 2015 Palermo [11] proposed an approach to account for very insufficient experimental data about the materials mechanical properties of the tower and provided a series of numerical simulations carried out on models with increasing levels of complexity.

2. Theoretical framework and methodology

During the last decade, the technological advances in engineering have made possible to obtain a large amount of information

about existing masonry structures. The Ground Penetrating Radar GPR methodology and the Terrestrial Laser Scanning TLS procedures are just two examples of the new methodologies applied to acquire a further and richer understanding of the Asinelli tower's actual state. The high precision of the method has permitted to obtain very precise measurements of the inclination and tilt, elevation drawings, presence of cracks and a 3D-point model of the tower [12,13].

This great amount of information allows, in principle, for the implementation of increasingly detailed three-dimensional numerical models. However, it is not straightforward assessing which is the optimal level of complexity that should be achieved. The present study aims to give some useful hints in order assess this issue when studying historical masonry towers.

This purpose will be fulfilled by comparing a series of three-dimensional models from simple to complex-shaped structures of the Asinelli tower, and with an increasing discretization (mesh) refinement. The numerical results will be compared with recent experimental measurements and with numerical results of one, two and three-dimensional models of the Asinelli tower achieved by different Authors in the last decades. The numerical modeling has been performed with the finite element code Diana (Diana BV, The Netherlands) and with the pre-post processor MIDAS FX+ for DIANA [14].

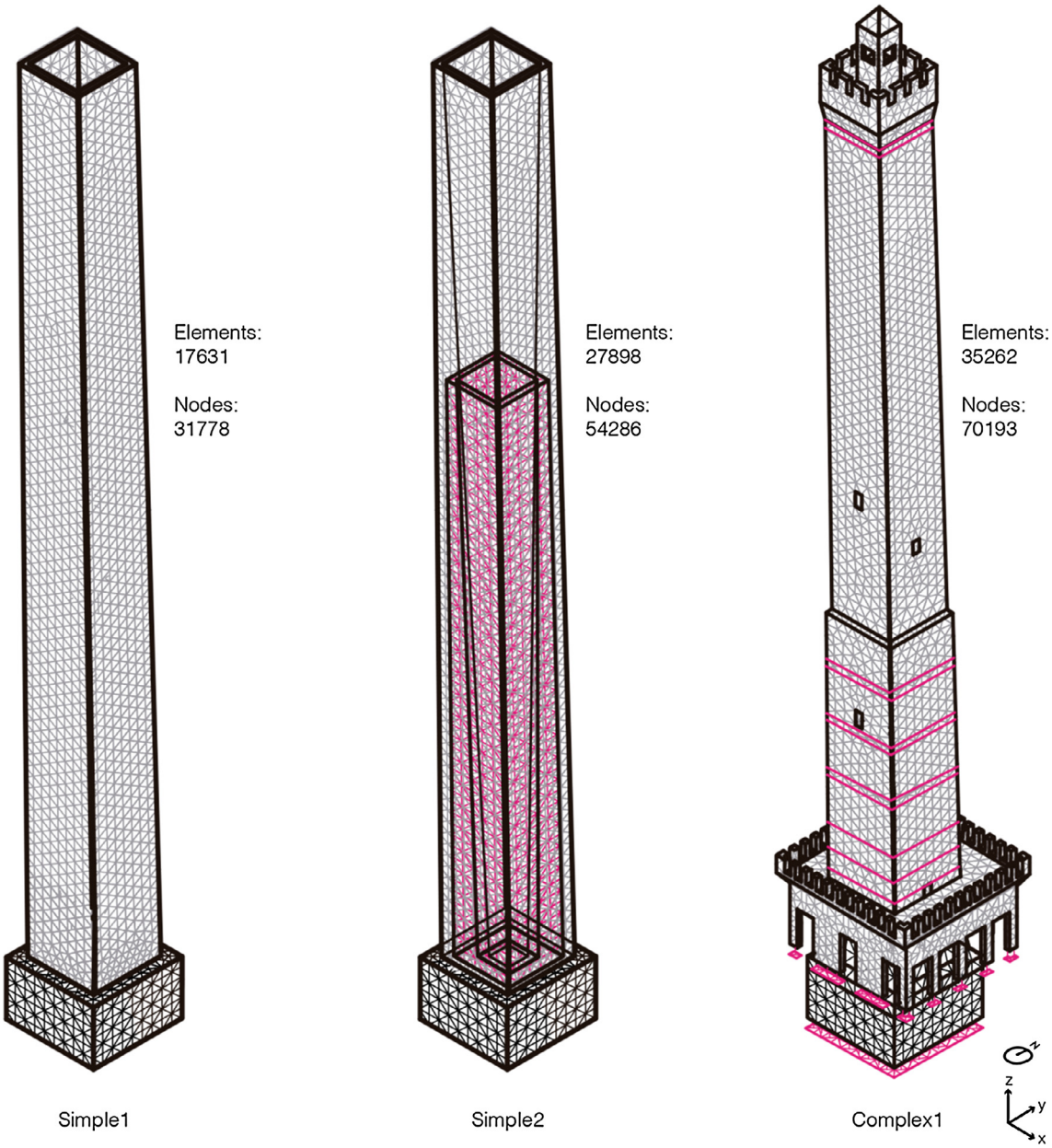

Fig. 2. *Simple*1, *Simple*2 and *Complex1* models.

2.1. Solid finite element models

Three solid finite element models with different levels of complexity are created for comparison. The first model, named *Simple1*, is the simplest one of all three, and is analogous to a previous structural modeling study [4]. The geometrical model of the emerging tower is basically a 98 m high hollow trunk that tapers from an 8 m-side squared cross-section at the bottom to a 7 m-side one at the top. The foundation is made of a quadrangular prism of approximately 10.5 m in the sides and 6.5 m in depth. The second model, named *Simple2*, is analogous to the previous but explicitly accounts for the brick-and-rubble walls in segments A, B and C of the tower. The foundation has the same dimensions as the Simple1 model. Finally, the third model, named *Complex1*, is modeled in order to be as close to the real tower as possible. In fact, it accounts for the rubble infill, the window openings in the walls (simple rectangle section), the belfry, the reinforcement cables and the portico. The foundation, as in reality, is divided in a selenite-stone base and a conglomerate quadrangular prism underneath. It is worth noting that all models include the real tilt and overhang (1.51° and 2.38 m respectively).

For the solid element mesh, ten-node quadratic isoparametric solid tetrahedron element (CTE30) is used [14]. This choice provides best performance in term of meshing simplicity, especially when geometry complexity increases, and efficiency, when material nonlinearity and strain localization id considered. This choice is the more effective also when automatic adaptive mesh refinement is required. Although the mean mesh element size is equal to 1.15 m for all three models, the increase of complexity involved a sensible increase in the number of elements and nodes. The three meshes are shown in Fig. 2.

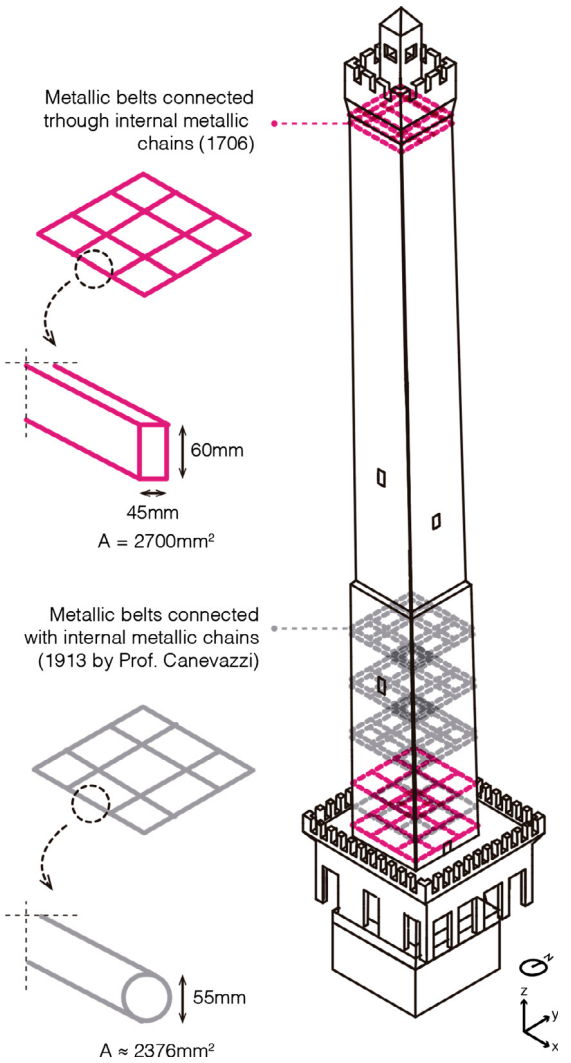

Fig. 3. Steel cables position and section dimensions.

2.2. Bar in solid elements

In the *Complex1* model, the reinforcement cables and chains are modeled as one-dimensional "bar in solid" or "reinforcement" elements [14]. These particular elements work as embedded lines with location and integration points in the solid element. Fig. 3 shows the position and dimensions of each reinforcement element used in the *Complex1* model.

2.3. Soil-structure interaction: The Winkler model

For the *Complex*1 model, the soil-structure interaction is also accounted for, by means of surface interface elements. This structural surface is obtained as a degeneration of solid elements and works as a Winkler model with shear stiffness. The adopted CT36I is a 6 + 6 node triangular surface quadratic element [14]. This element is concordant with the CTE30 solid element adopted to model the continua. Fig. 4 shows a detail of the foundations modeled with surface elements, where the thickness of the interface has been increased for clarity.

2.4. Numerical simulation of preexisting cracks and damage

Since the construction, the Asinelli tower has been subjected to a number of damaging events, including seismic events, fires, etc. [1,2]. Therefore, the masonry nowadays presents a diffuse subvertical cracking pattern [8]. The presence of this damage does not affect considerably the distribution of vertical stresses, but it does affect the dynamic behavior of the tower, as will be demonstrated in the following. It is worth noting that damage induced anisotropy is often more relevant than that due to the masonry texture anisotropy itself.

In order to account for this phenomenon in a simple but effective way, an original approach is proposed, based on an analogy with the so called smeared crack model [15].

This model decomposes the total strain ε into an elastic strain ε^e and a crack strain ε^{cr}, as follows:

$$\varepsilon = \varepsilon^e + \varepsilon^{cr}. \tag{1}$$

This crack strain sub-decomposition allows the modeling of a series of cracks that occur simultaneously, considering that a stress σ_i and strain ε_i^{cr} exist in a $n-t$ coordinate system aligned with each crack i. For simplicity, Fig. 5 illustrates this concept in the plane case, but three-dimensional generalization is straightforward.

In this way, the vector that assembles each individual crack strain denoted by ε^{cr}, the crack strain for each crack i given by ε_i^{cr} and the relation between global strain and local strain (affected by the transformation matrix N) are calculated as:

$$\varepsilon^{cr} = [N_1, N_2, \ldots, N_i, \ldots, N_N] \cdot \langle \varepsilon_1^{cr}, \varepsilon_2^{cr}, \ldots, \varepsilon_i^{cr}, \ldots, \varepsilon_N^{cr} \rangle^T. \tag{2}$$

The constitutive relation for each crack i is determined by the softening relation that expresses the stress exchanged across the crack as a function of the crack opening displacement. In case of crack unloading, both crack normal strain and crack normal stress vanish. The secant stiffness parameters $D^{\mathrm{I}}_{secant} = \mu E/(1-\mu)$ and $D^{\mathrm{I}}_{secant} = \beta G/(1-\beta)$ can be translated into traditional reduction factors as follows:

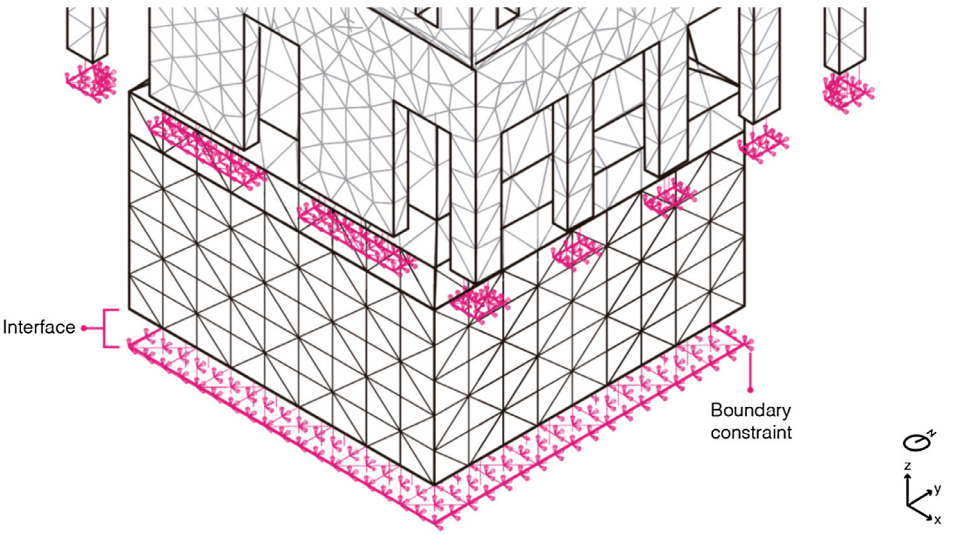

Fig. 4. Interface element in *Complex1* model with boundary constraints.

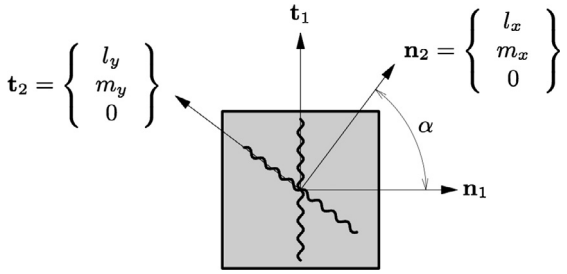

Fig. 5. Multi-directional fixed crack model for plain strain [14].

$$\begin{Bmatrix} \sigma_{xx} \\ \sigma_{yy} \\ \tau_{xy} \end{Bmatrix} = \begin{bmatrix} \frac{\mu E}{1-\mu\nu^2} & \frac{\mu\nu E}{1-\mu\nu^2} & 0 \\ \frac{\mu\nu E}{1-\mu\nu^2} & \frac{E}{1-\mu\nu^2} & 0 \\ 0 & 0 & \frac{\beta E}{2(1+\nu)} \end{bmatrix} \begin{Bmatrix} \varepsilon_{xx} \\ \varepsilon_{yy} \\ \gamma_{xy} \end{Bmatrix}, \tag{3}$$

where μ is the reduction factor of the Young's modulus E and β is the reduction factor of the shear modulus G. It is evident that, when cracking is not propagating further, Eq. (3) is basically an anisotropic elastic relation [16]. Although in principle the amount of damage induced anisotropy could be directly obtained from a very detailed crack survey, this procedure would be cumbersome, therefore a simplified approach is proposed. First of all, since the existing diffused cracking is mainly subvertical, a damage parameter d will be introduced, that accounts for the decrement of the Young modulus in the horizontal direction E_H with respect to the Young modulus in the vertical direction E_V which will be kept constant, as follows:

$$\frac{E_H}{E_V} = \frac{E_1}{E_3} = \frac{E_2}{E_3} = d \leqslant 1 \tag{4}$$

This parameter will modify the elastic coefficients of the brick and infill materials where the cracks are present, converting them in anisotropic materials. Since the parameter affects both horizontal directions in the same way, these materials will actually have a transversely isotropic elasticity, and its stiffness matrix will have just 5 unknowns. After some simplifications, the elastic stiffness matrix adopted for masonry becomes:

Table 1
Simple1, *Simple2* and *Complex1* models material properties (* assumed values).

Material			*Simple1*	*Simple2*	*Complex1*
Reference			[18]	[11]	[11]
Walls	Brick	E [N/m^2]	5E+09	4E+09	4E+09
		Mass density [N/m^3/g]	1800	1700	1700
		ν	0.2	0.2	0.2
	Rubble infill	E [N/m^2]	–	3E+09	3E+09
		Mass density [N/m^3/g]	–	1600	1600
		ν	–	0.2	0.2
Foundation	Selenite stone	E [N/m^2]	5E+09	4E+09	4E+09
		Mass density [N/m^3/g]	1800	2200	2200
		ν	0.2	0.2	0.2
	Conglomerate	E [N/m^2]	–	–	5E+09*
		Mass density [N/m^3/g]	–	–	1800*
		ν	–	–	0.2
	Soil	k_n, k_t [N/m^3]	–	–	Variable
Other	Cables	E [N/m^2]	–	–	2E+11*
		Mass density [N/m^3/g]	–	–	7850
		ν	–	–	0.3*

$$[H]^{-1} = \begin{bmatrix} \frac{1}{E_1} & \frac{-\nu_{21}}{E_2} & \frac{-\nu_{31}}{E_3} & 0 & 0 & 0 \\ \frac{-\nu_{12}}{E_1} & \frac{1}{E_2} & \frac{-\nu_{32}}{E_3} & 0 & 0 & 0 \\ \frac{-\nu_{13}}{E_1} & \frac{-\nu_{23}}{E_2} & \frac{1}{E_3} & 0 & 0 & 0 \\ 0 & 0 & 0 & \frac{1}{G_{12}} & 0 & 0 \\ 0 & 0 & 0 & 0 & \frac{1}{G_{23}} & 0 \\ 0 & 0 & 0 & 0 & 0 & \frac{1}{G_{13}} \end{bmatrix} = \begin{bmatrix} \frac{1}{dE_V} & \frac{-\nu}{dE_V} & \frac{-\nu}{E_V} & 0 & 0 & 0 \\ \frac{-\nu}{dE_V} & \frac{1}{dE_V} & \frac{-\nu}{dE_V} & 0 & 0 & 0 \\ \frac{-\nu}{dE_V} & \frac{-\nu}{dE_V} & \frac{1}{E_V} & 0 & 0 & 0 \\ 0 & 0 & 0 & \frac{2(1+\nu)}{dE_V} & 0 & 0 \\ 0 & 0 & 0 & 0 & \frac{2(1+\nu)}{E_V} & 0 \\ 0 & 0 & 0 & 0 & 0 & \frac{2(1+\nu)}{E_V} \end{bmatrix} \tag{5}$$

It is worth noting that the accounting for diffused vertical cracking damage with the proposed simplified approach requires only for the d extra parameter. If $d = 1$ the masonry is undamaged and the elastic constitutive law is isotropic. In the following d will be determined as a dynamic identification parameter to be determined from best fitting of experimental results, paying attention that relevant fundamental inequalities among the different Young modulus and Poisson coefficients are verified [17].

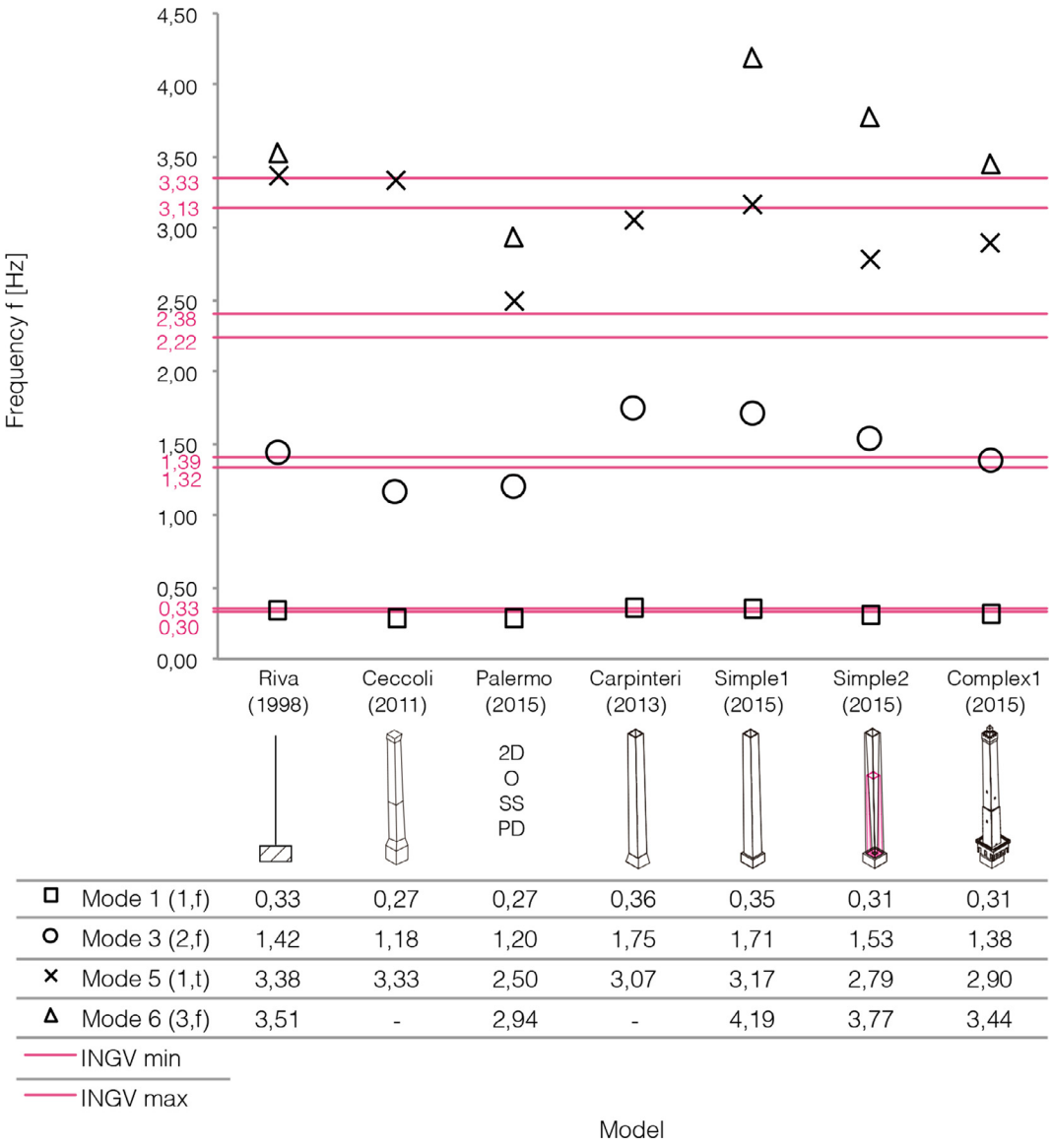

□	Mode 1 (1,f)	0,33	0,27	0,27	0,36	0,35	0,31	0,31
○	Mode 3 (2,f)	1,42	1,18	1,20	1,75	1,71	1,53	1,38
×	Mode 5 (1,t)	3,38	3,33	2,50	3,07	3,17	2,79	2,90
△	Mode 6 (3,f)	3,51	-	2,94	-	4,19	3,77	3,44
—	INGV min							
—	INGV max							

Fig. 6. Comparison between numerical models and experimental results (INGV range [19]).

3. Numerical results and discussion

3.1. First comparison: Linear static analysis

The first comparison will use all three models with isotropic materials (i.e. parameter $d = 1$) to account for differences in the geometry complexity and refinement of the model. Table 1 shows the values of the materials' properties used and the corresponding reference.

The *Simple1* model will be based on the materials from [18], whilst the *Simple2* and *Complex1* model will be based on [11]. Since not all of the materials elastic properties values were available, standard values according to the type of material were selected when necessary to be able to perform adequately the further analyses.

The maximum elastic displacement for the *Simple1*, *Simple2* and *Complex1* is found at the top with values of 0.085 m, 0.108 m and 0.119 m respectively. The displacement value and shape of the *Simple1* model agree entirely with the one found in previous studies [18] in which a very similar model was studied in terms of shape complexity and materials. The results of the *Simple2* and *Complex1* model are still very similar and concordant with this previous result.

As far as vertical stresses in the masonry is concerned, large compression stresses (negative values) are local and in correspondence with the maximum inclination (West) facade, as it was expected from a self-weight structural analysis. *Simple1* presents the lowest and more uniform values, while *Complex1* has the highest and more localized vertical stresses. This fact can be explained due to higher complexity and detailing of the solid elements and mesh refinement. This result agrees with previous research in which the larger values of vertical stress were found in the lower west part of the tower [18]. This region of the tower, as a consequence, has

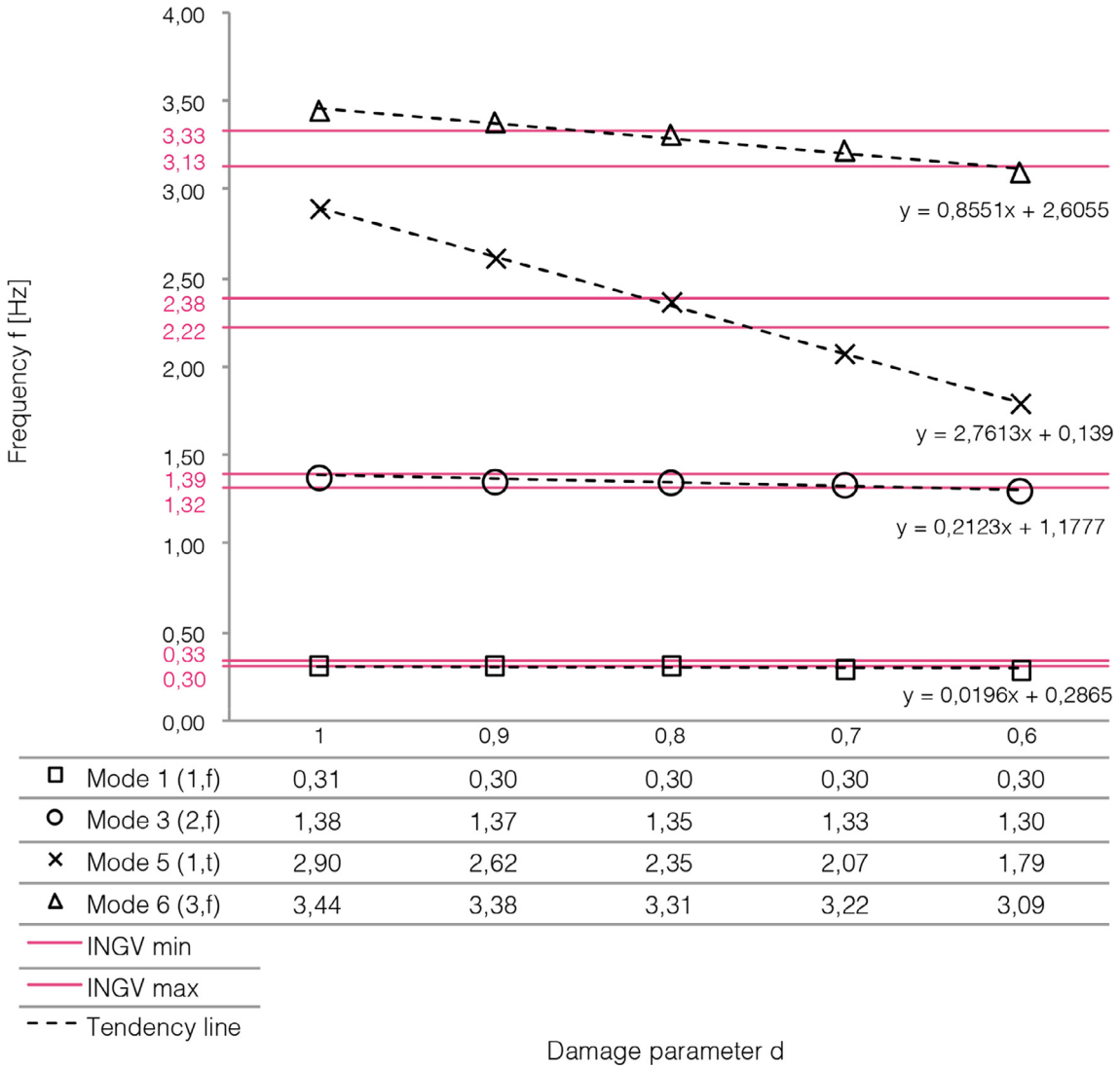

Fig. 7. Frequencies for different damage parameters (Mode 1, 3, 5 and 6).

always deserved special attention both as preferential location for acoustic emission monitoring [10,18,19] and for retrofitting interventions to confine the large vertical stress and minimize the structural decay.

3.2. Modal analysis

As a first step, modal analysis was carried out assuming isotropic materials ($d = 1$), in order to compare the three models (*Simple1*, *Simple2* and *Complex1*) with experimental and numerical results available in the literature. The comparison considered the first six natural frequencies and modal shapes. Note that mode 1 and 2, as well as 3 and 4 basically refer to the same bending phenomena of the tower in the two orthogonal directions. Although the symmetry of the tower is not perfect, due to the presence of openings and other details, each couple of bending modes will be considered as one for the sake of simplicity, also in the *Complex1* model.

In Fig. 6 the frequencies of the first 3 bending modes (Modes 1, 3 and 6) and the first torsional mode (Mode 5) are compared to other numerical [5,7,11] and experimental [19] results of the previous models achieved. In general, all models are in quite good agreement with the real response.

The Riva [7] beam model agrees well in the response of the first two bending modes. However, the following modes have frequencies with higher values than the real response. Similarly, the Ceccoli [5] shell model, fits well the first mode in the experimental ranges, but not for the higher ones. The 2D-O-SS-PD shell model by Palermo [11] fits better the 4 modes studied, but in order to lower and improve the value calculated for the torsional frequency, the mechanical parameters were identified in a way such that also the bending frequencies were consequently lowered. Carpinteri three-dimensional model [18] and *Simple1* model of this study provide very similar frequencies. This result was expected since both geometry and material properties are very similar. Both models provide good estimate of the first couple of modes, similarly to Riva [7] and Ceccoli [5] models.

Apparently, accurate results do not strictly depend on full solid modeling. In fact, Palermo [11] shell model is more successful in higher natural frequency simulation than the simpler three-dimensional models (Carpinteri [18] and *Simple1*).

However, when three-dimensional models detailing and material properties accuracy increase, the results get closer to the experimental measurements. The tendency between *Simple1*, *Simple2* and *Complex1* model show clearly this aspect. *Simple 2*, which includes the rubble infill and experimentally taken material properties, is an even better approximation of the response, with higher frequencies very close to the INGV interval [19]. The highest complexity model *Complex1* arrives at real frequencies with the best accuracy of all. The bending modes frequencies are practically all inside or very close to be in the INGV ranges. Nevertheless, its torsional mode frequency is almost a 20% out of the real torsional response.

Even if Palermo's model has accurate results that are comparable with the *Complex1* response, it considers orthotropic masonry to arrive better at the torsional response but sacrificing the bending response.

As a second step, in order to improve the ability of the proposed *Complex1* model in capturing the first torsional modal frequency, the preexisting subvertical cracking of the tower is modeled by decreasing the d damage parameter previously introduced.

As d is diminished, starting from 1 (undamaged, isotropic masonry) down to 0.6, all the calculated natural frequencies decrease, which is intuitive since stiffness is decreased, but with very different trends. All the bending natural frequencies, and in particular the first two, are almost unaffected by the damage increase (lowering of d parameter). On the contrary, the decrement of the torsional frequency is sensible. From a theoretical point of view, this makes sense since the tower is basically a hollow core vertical cantilever. Therefore, the bending stiffness highly depends on the longitudinal Young's modulus, that remains constant, while the torsional stiffness highly depends on circumferential (with respect to the tower longitudinal axis) shear modulus which is diminished d times.

Fig. 7 shows this phenomenon in a clear way. The frequency f has been plotted for each damage parameter d chosen in this study (from 1.0 to 0.6). The tendency line approximate equation has been calculated and shown in the figure for modes 1, 3, 5 and 6 (three bending modes and one torsional mode). The slopes on each equation show clearly that the bending modes frequencies (slopes 0.0196, 0.2123 and 0.8551 for modes 1, 3 and 6 respectively) decrease in a lower rate than the torsional mode period (2.7613 slope) while changing the damage parameter.

It is evident that damage values in between $d = 0.8$ and $d = 0.7$ are the parameters that allow the numerical calculation of the frequencies that better approximate the experimental measurements. Although further bisection iterations are possible, the results obtained in correspondence of $d = 0.8$ is already a very good approximation. This parameter indicates that vertical cracking in the Asinelli tower decreases the horizontal stiffness by approximately a 20%.

The results from this comparison show that anisotropic modeling of the materials display a much accurate modal response than isotropic modeling when cracking is present in the actual construction. This aspect is extremely relevant in the structural assessment of existing structures, since the percentage of damaging is important and the variation of the material characteristics on each direction could be of a greater relevancy.

3.3. Nonlinear static analysis (Pushover)

In this section the *Simple1*, *Simple2* and *Complex1* models will be compared in term of nonlinear static pushover analysis response. The materials are considered isotropic, according to the mechanical parameters listed in Table 1. When additional values were necessary for the nonlinear analysis, they were collected from the literature [7,8,11,18]. The comparison parameters will be the Modal pushover analysis (MPA) [20] curves of each model, the reduction factor q and the ultimate state of the masonry material (cracking pattern).

With this procedure is possible to obtain a better understanding of the efficiency of each type of model in performing an analysis that takes into account the nonlinearity in geometry and masonry material (including brick and rubble infill) and effectiveness in

generating accurate results of the Asinelli tower's seismic capacity.

Fig. 8 shows the comparison between the pushover curves (top displacement against base shear) of the three models.

From the three initial capacity curves, it is clear that an increment on modeling detailing decreases the yield force and maximum force that the tower resists. This means that over simplified three-dimensional model might overestimate the capacity of the structure and generate larger values than the actual seismic response of the tower. Furthermore, the *Complex1* capacity curve is smoother than the others probably due to the explicit presence of opening and other reentrant corners, that act as multiple fracture propagation sources providing a more ductile failure mechanism (see Table 2).

On the other hand, *Simple1* and *Simple2* models have a very similar maximum displacement D_u, while *Complex1* model has a larger one. These displacements are larger than those found in the linear analysis. In a similar way, *Simple1* model has the lowest yield displacement, whilst *Complex1* has the highest one, indicating that yielding occurs at increasing deformations for the three models, and that yielding is more gradual for the last model.

According to the Italian standards [21], the reduction factor for the Asinelli tower can be estimated equal to 2.8, on the base of the main stiffness changes in height, of the material variability and of the structural wall type. Alternatively, the reduction factor can be assessed numerically from a bilinear approximation of the capacity curves [20]. The calculated reduction factors for the three models studied are quite lower than the estimated one and have a tendency to decrease when the model complexity increases.

Therefore, increasing model complexity, accounting for refined geometry, soil-structure interaction, openings and portico modeling, reinforcements and material properties based on experimental tests values, is portraying a lower capacity than expected by the national code.

Fig. 9 shows the nonlinear cracking patterns for each model, in correspondence to the last step of the pushover analysis.

Simple1 model provides a very localized cracking pattern. As a consequence, the failure mechanism resembles a rigid collapse and the upper part of the tower changes its inclination abruptly. A more diffuse cracking pattern is found for *Simple2* model, with better detectable shear bands in addition to flexural cracking. Nevertheless, *Simple1* and *Simple2* crack patterns are quite similar one to each other.

Nonlinear static analysis provides a much more different cracking pattern for *Complex1* model. Cracking energy distributes in a much realistic way, since various discontinuities on the model have been modeled: openings, merlons, belfry, and so on. In the lower part of the tower, the portico slab cracking propagates from the very beginning of the analysis, together with the tension wall of the tower. The columns of the portico show larger damage in the tension side and a concentrated damage in the compression side. Localized areas begin to damage also close to the retrofitting reinforcements, meaning masonry is being crushed on the compression side of the tower. Afterwards, in the first third of the tower, where an abrupt change of rigidity exists, a cracking pattern is also developed. Right in the horizontal ring where the change of rigidity is located, the masonry is very damaged. Next to window openings, a series of cracks is also shown. This failure mechanism explains the more gradual transition in the pushover capacity curve and also the lower maximum force.

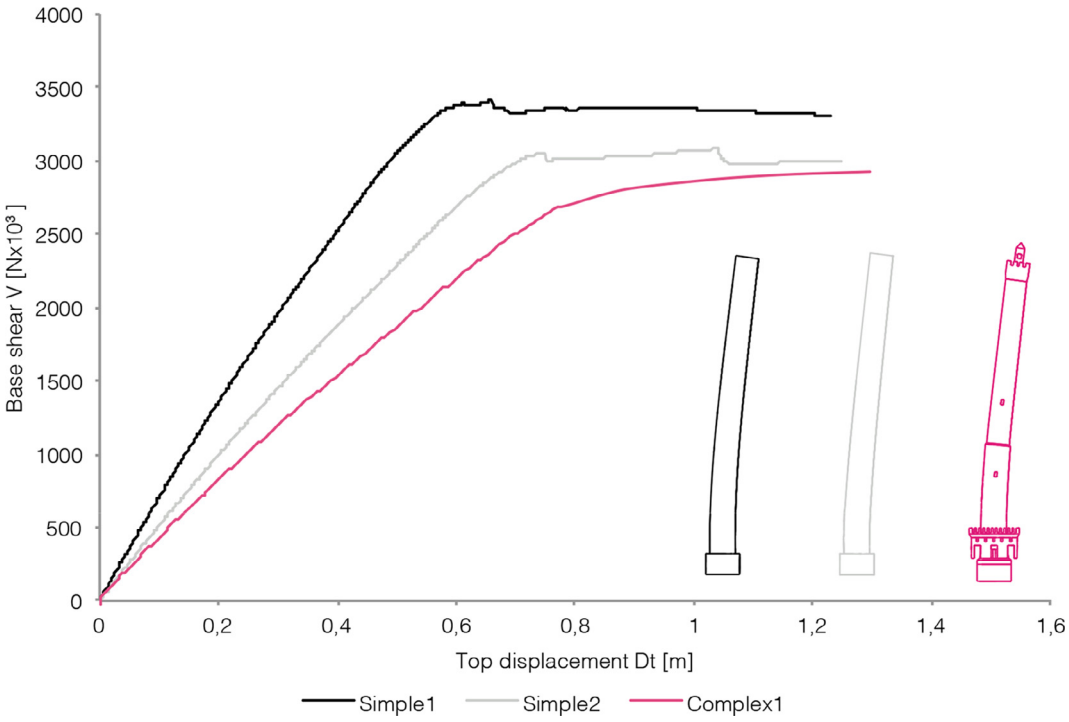

Fig. 8. Pushover curves for *Simple1*, *Simple2* and *Complex1* models.

Table 2
Lists the reduction factors calculated according to the bilinear equivalent SDOF curves found.

Model	Reduction factor q
Simple1	2.30
Simple2	1.88
Complex1	1.69

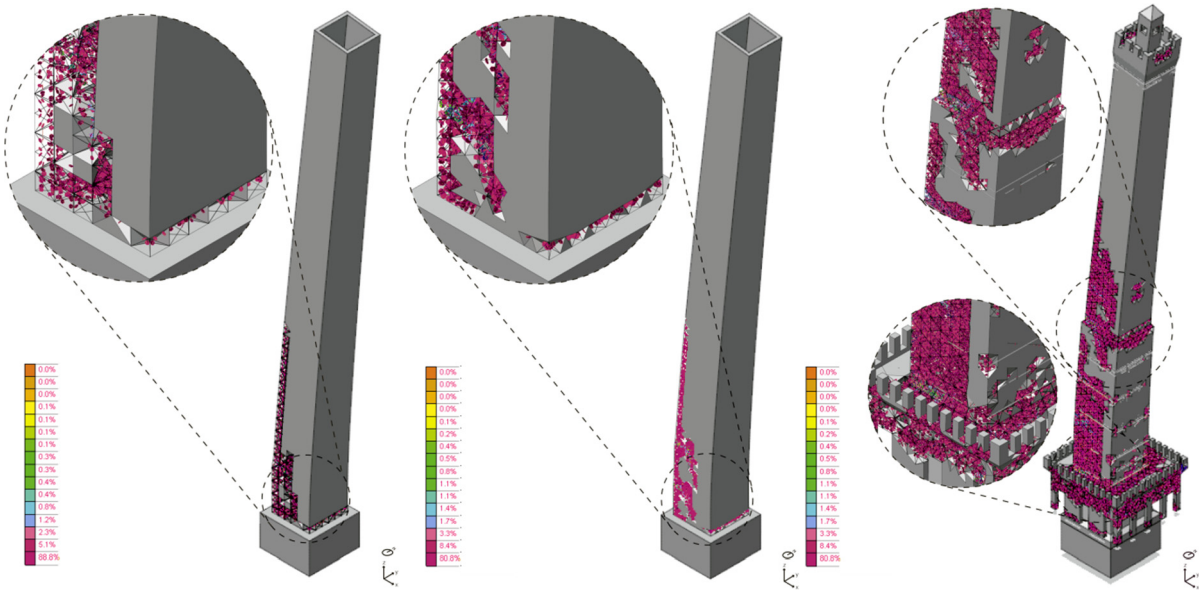

Fig. 9. *Simple1*, *Simple2* and *Complex1* nonlinear cracking patterns.

The numerical crack pattern suggests which position is more relevant when Acoustic Emission monitoring is foreseen and sensor positioning has to be planned [9]. In literature the AE phenomenon has been numerically modeled following different approaches, depending on the scale and on the aspects of the problem under consideration [22–25]. Upon fracture mechanics description, different source hypotheses have been proposed on the crack propagation models, numerically connecting crack advancements to the occurrence of acoustic emission [26–29].

In this case it is interesting to observe how the location of propagating cracks due to horizontal seismic accelerations is in agreement with the choice adopted for the monitoring campaign described in the following section [18].

4. Acoustic emission monitoring

In the present section, an investigation of causal relationships between AE bursts and environmental local phenomena such as earthquakes, wind and vehicle traffic intensity is proposed.

The AE monitoring lasted about 4 months starting from the end of September 2010 to the end of January 2011. Six piezoelectric sensors were attached to the northeast corner of the tower at an average height of ca. 9.00 m above ground level, immediately above the terrace atop the arcade [30]. The numerical simulation presented above proved that the choice of this location optimizes the chance of acquiring acoustic emission from ongoing cracking phenomena. In this region of the tower, the thickness of the double-wall masonry is equal to 2.45 m approximately. The monitoring of the most relevant zone of the tower allowed for the assessment of the damage evolution. The analysis of the results allowed also to assess the relative influence of the main actions, namely: the vehicle traffic, the seismic activity [30] and the wind thrust.

During the monitoring period, the strongest earthquakes were the 4.1 magnitude event that occurred on 13 October 2010 at 11:43 p.m. in the Rimini area (epicenter about 100 km from Bologna) and the 3.4 magnitude event on 21 November 2010 at 4:10 p.m. in Modena Apennines (epicenter about 50 km from Bologna).

According to the authors' experience, in order to filter out environmental background noise in masonry, the detection threshold of the sensors was set equal to 100 mV [31–33]. Both the arrival time, determined by using the first threshold crossing of the signal, and the peak amplitude V_{max} (expressed in μV), which defines the magnitude of the AE event as $M = log(V_{max}/1\,\mu V)$, were stored continuously during the monitoring period.

There appears to be a significant correlation in time between AE activity in the tower and local seismicity, as the Rimini

earthquake apparently triggered the largest AE burst, thus resulting in the highest damage effect on the tower; the about 3000 AE events detected in the first 12 h after the earthquake account for the 25% of 14 400 events collected during the entire monitoring period.

On the other hand, there is an evidence of seismic events which followed AE bursts and, therefore, did not trigger acoustic emissions from the tower. In particular, the seismic sequence between 1700 and 1800 h apparently occurred as the culmination of a 10-day period of intense AE activity.

Such AE bursts may indicate crustal stress releases affecting large areas during the preparation of a seismic event, as supported by several case histories from Italy, where an increased AE activity was observed before strong earthquakes.

However, a rigorous investigation on causal relationships between AE bursts and earthquakes would require a simultaneous operation of suitable arrays of AE monitoring sites, adequately placed in the territory, e.g., over a large regional area.

The *b*-value is an important parameter for damage assessment of structures as it decreases in case of damage evolution [34–36]. The time evolution of damage is captured as well by a time-scaling approach, $N(t) \sim t^{\beta t}$, where $N(t)$ is the accumulated number of AE events up until the time t and βt is a fitting parameter, which characterizes the damage evolution ($\beta_t > 1$ describes accelerated damage). The steady trend of *b*-value over time, plotted in Fig. 10(c), suggests that the wall experiences damage which can approach locally to conditions of instability (*b*-value < 1.0) [34–36].

The presented monitoring campaign provided also a way to assess the potential harm of heavy vehicle traffic passing nearby the tower in the Bologna's historic center. The vibrations induced by traffic to the surrounding buildings are mainly due to the relatively high-speed passage of heavy vehicles over roads with uneven surface profile. The interaction between the wheels and the road surface

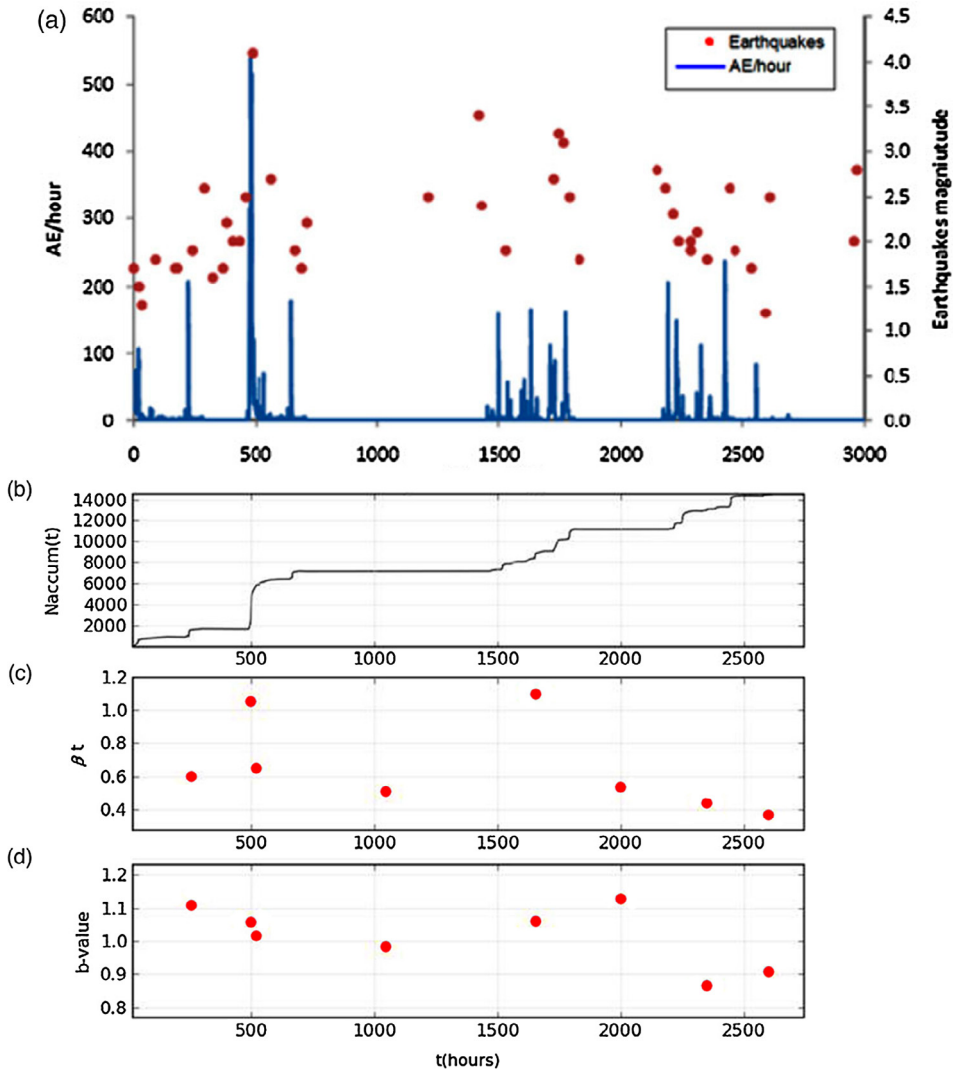

Fig. 10. Damage assessment of the Asinelli Tower: AE per hour and earthquake magnitude (a) [10]; accumulated number of AE events as a function of time (b); *b*-value and β_t trends over time during the entire monitoring period: *b*-values and β_t are calculated with using groups of 2000 AE events (c and d) [30].

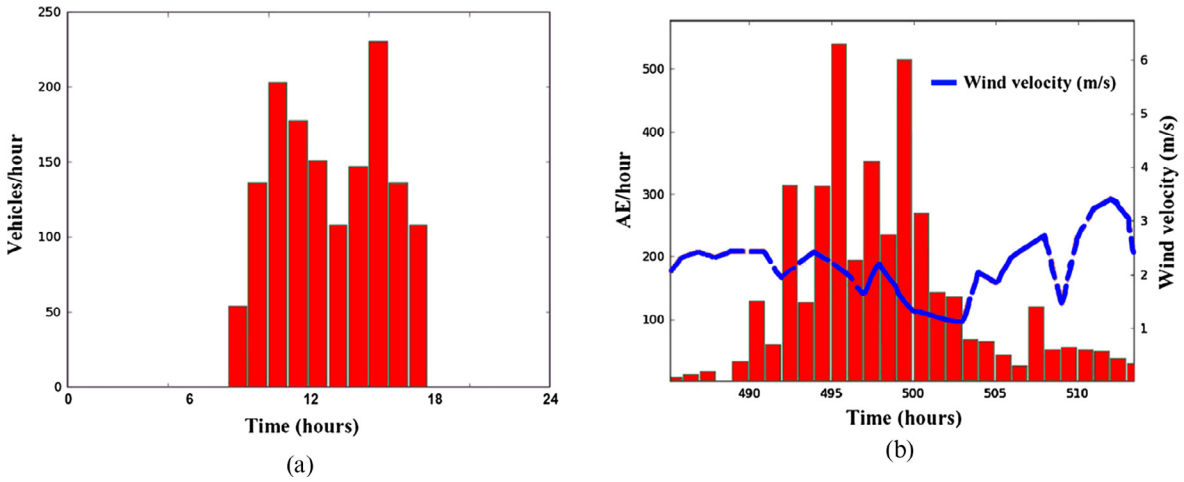

Fig. 11. Vehicle volume week distributions in the areas surrounding the Asinelli Tower (a); Instantaneous AE rate and wind speed (b).

causes mechanical waves propagation in the soil down to the foundations of nearby structures.

Fig. 11a shows the vehicle volume per hour recoded during one week in the areas surrounding the Asinelli Tower including mass transit, private, and heavy vehicles, from 8 AM to 6 PM. This recursive phenomenon shows no correlation with AE cumulative distribution (Fig. 10a) which is characterized by wide silent periods in between very localized AE bursts.

A sensor for the acquisition of wind speed was applied to the tower at a height of approximately 78 m above the ground. The measured wind speed ranged between 1 and 7 m/s. These values appear unable to generate sensible aerodynamic loads on the tower. This is confirmed by the lack of correlation between wind intensity and AE activity in the tower, as shown in Fig. 11b.

5. Conclusions

The finite element method has been used to model and analyze the most emblematic masonry tower in Bologna, Italy: the Asinelli tower.

Thanks to modern laser survey technologies and non-destructive techniques, three different finite element structural models of the tower have been constructed, each one characterized by increasing geometrical details, and by increasing complexity of the adopted material modeling.

The structural response of the three models has been assessed in terms of both linear static analysis and modal analysis. In addition, a gradually decreasing damage parameter d is used as a multiplier of the transversely isotropic elastic coefficients in the masonry, to study the effect of preexisting vertical cracks found in the most recent studies for the conservation and restoration of the tower. Finally, the nonlinear static analysis (pushover) has been performed, accounting for mechanical and geometrical non-linearities.

The numerical comparisons show that the simpler models are able to reproduce correctly only some basic features of the tower, as vertical stresses, top displacements and the first modal frequency. On the contrary, the most detailed model better performs from several points of view, especially if preexisting damage anisotropy is properly taken into account. Moreover, nonlinear analyses reveal that simpler models provide overestimated structural reduction factors.

The AE monitoring takes benefits of numerical simulations both in the design phase (optimal sensor placing) and for the interpretation of results. The AE monitoring is useful to assess the integrity of the Tower with respect to different potential source of damage, allowing for discrimination among the most harmful actions.

Acknowledgements

Lozano-Ramírez acknowledges the fellowship from Colfuturo and Pontificia Universidad Javeriana, Bogotá, Colombia, to pursue a Master's degree at Politecnico di Torino [37].

The technical support of Diana FEA BV during the course of this study is gratefully acknowledged.

The authors wish to thank the Municipality of Bologna and Eng. R. Pisani for allowing this study on the Asinelli Tower.

This research received no specific grant from any funding agency in the public, commercial, or not-for-profit sectors.

Appendix A. Supplementary material

Supplementary data associated with this article can be found, in the online version, at http://dx.doi.org/10.1016/j.engfracmech.2018.05.011.

References

[1] Savioli LV. Annali Bolognesi, vol. 3. Bologna: Bassano Remondini e figli; pp. 1784–1795.
[2] Cavani F. Sulla pendenza e sulla stabilità della Torre degli Asinelli di Bologna. Bologna: Accademia delle Scienze; 1912.
[3] Capitani O. Bologna nel Medioevo. Bologna: Bononia University Press; 2007.
[4] Carpinteri A, Lacidogna G, Manuello A, Niccolini G. A study on the structural stability of the Asinelli Tower in Bologna. Struct Control Health Monit 2016;23:659–67. http://dx.doi.org/10.1002/stc.
[5] Comune di Bologna, Bologna città delle torri: attraverso la storia, l'arte e la tecnica. Bologna: CIPEA; 2009.
[6] Comune di Bologna. Progetto per il consolidamento delle strutture in elevazione della torre Asinelli [Technical sheets TAV1a - 4b]; 2010.
[7] Riva P, Perotti F, Guidoboni E, Boschi E. Seismic analysis of the Asinelli Tower and earthquakes in Bologna. Soil Dyn Earthq Eng 1998;17(7–8):525–50.
[8] Comune di Bologna. Monitoraggio Due Torri. Iperbole: La rete civica di Bologna; 2012.
[9] Invernizzi S, Lacidogna G, Carpinteri A. Numerical models for the assessment of historical masonry structures and materials, monitored by acoustic emission. Appl Sci 2016;6:102. http://dx.doi.org/10.3390/app6040102.
[10] Lacidogna G, Cutugno P, Niccolini G, Invernizzi S, Carpinteri A. Correlation between earthquakes and AE monitoring of historical buildings in seismic areas. Appl Sci 2015;5:1683–98. http://dx.doi.org/10.3390/app5041683.
[11] Palermo M, Silvestri S, Gasparini G, Baraccani S, Trombetti T. An approach for the mechanical characterisation of the Asinelli Tower (Bologna) in presence of insufficient experimental data. J Cult Herit 2015;16(4):536–43. http://dx.doi.org/10.1016/j.culher.2014.05.002.
[12] Bertacchini E, Boni E, Capra A, Castagnetti C, Dubbini M. Terrestrial laser scanner for surveying and monitoring middle age towers. In: Proceedings of the XXIV FIG Congress - Facing the Challenges-Building the Capacities, Sidney, Australia; 2010, TS 4D – TLS Application I 4445.
[13] Pesci A, Teza G, Bonali E, Casula G, Boschi E. A laser scanning-based method for fast estimation of seismic-induced building deformations. ISPRS J Photogramm Remote Sens 2013;79:185–98. http://dx.doi.org/10.1016/j.isprsjprs.2013.02.021.
[14] Diana FEA BV, DIANA - Finite Element Analysis User's Manual, Manie J, editor. DIANA FEA BV Delftechpark 19a, 2628 XJ Delft, The Netherlands.
[15] Rots JG, Blaauwendraad J. Cracks models for concrete: discrete or smeared? Fixed, multi-directional or rotating? Heron 1989;34(1):3–33.
[16] Rots JG, Invernizzi S, Belletti B. Saw-tooth softening/stiffening – a stable computational procedure for RC structures. Comput Concr 2006; 3(4).
[17] Carpinteri A. Structural mechanics fundamentals. Boca Raton: CRC Press Taylor & Francis; 2014.
[18] Carpinteri A, Lacidogna G, Invernizzi S, Manuello A. AE monitoring and structural modeling of the Asinelli Tower in Bologna. In: Proceedings of the 13th International Conference of Fracture, Beijing, China; 2013. p. 10.
[19] Azzara RM, Cavaliere A, Danesi S, Morelli A, Zaccarelli L. Rapporto Tecnico 284: Il monitoraggio sismico della torre degli Asinelli e della Garisenda. Risultati preliminari dell'analisi dei dati", Istituto Nazionale di Geofisica e Vulcanologia INGV, Roma; 2014. p. 284.
[20] Chopra AK, Goel RK. A modal pushover analysis procedure for estimating seismic demands for buildings. Earthquake Eng Struct Dyn 2002;31:561–82.
[21] Direttiva del Presidente del Consiglio dei Ministri 9 febbraio 2011. Valutazione e riduzione del rischio sismico del patrimonio culturale con riferimento alle Norme tecniche per le costruzioni di cui al D.M. 14/01/2008. Gazzetta Ufficiale n. 47 26/02/2011 - suppl. ord. n. 54.
[22] Onoe M, Tsao JW. Numerical simulation of acoustic emissions. Jpn J Appl Phys 1981;20:177–80.
[23] Sause MRG, Richler S. Finite element modelling of cracks as acoustic emission sources. J Nondestruct Eval 2015;34.
[24] Tang C. Numerical simulation of progressive rock failure and associated seismicity. Int J Rock Mech Min Sci 1997;34:249–61.
[25] Grégoire D, Verdon L, Lefort V, Grassl P, Saliba J, Regoin JP, et al. Mesoscale analysis of failure in quasi-brittle materials: comparison between lattice model and acoustic emission data. Int J Numer Anal Meth Geomech 2015;39:1639–64.
[26] Mpalaskas AC, Vasilakos I, Matikas TE, Chai HK, Aggelis DG. Monitoring of the fracture mechanisms induced by pull-out and compression in concrete. Eng Fract Mech 2014;128:219–30.
[27] Ohtsu M, Kaminaga Y, Munwam MC. Experimental and numerical crack analysis of mixed-mode failure in concrete by acoustic emission and boundary element method. Constr Build Mater 1999;13:57–64.
[28] Schechinger B, Vogel T. Acoustic emission for monitoring a reinforced concrete beam subject to four-point-bending. Constr Build Mater 2007;21:483–90.
[29] Veselý V, Vodák O, Trčka T, Sobek J, Koktavý P, Keršner Z, et al. Acoustic emission from quasi-brittle failure of cementitious composites - Experimental measurements and cohesive crack model simulations. Key Eng Mater 2014;676–679.
[30] Carpinteri A, Lacidogna G, Manuello A, Niccolini G. A study on the structural stability of the Asinelli Tower in Bologna. Struct Control Health Monit 2016;23:659–67.
[31] Anzani A, Binda L, Carpinteri A, Invernizzi S, Lacidogna G. A multilevel approach for the damage assessment of historic masonry towers. J Cult Heritage 2010;11(4):459–70.
[32] Carpinteri A, Invernizzi S, Lacidogna G. In situ damage assessment and nonlinear modelling of an historical masonry tower. Engng Struct 2005;27:387–95.
[33] Carpinteri A, Invernizzi S, Lacidogna G. Numerical assessment of three medieval masonry towers subjected to different loading conditions. Masonry Int 2006;19:65–76.
[34] Carpinteri A, Chiaia B, Invernizzi S. Applications of fractal geometry and renormalization group to the Italian seismic activity. Chaos, Solitons Fractals 2002;14(6):917–28. http://dx.doi.org/10.1016/S0960-0779(02)00081-4.
[35] Colombo S, Main IG, Forde MC. Assessing damage of reinforced concrete beam using "b-value" analysis of acoustic emission signals. J Mater Civ Engng ASCE 2014;15:280–6. http://dx.doi.org/10.1061/(ASCE)0899-1561(2003) 15:3(280).
[36] Carpinteri G, Lacidogna Puzzi S. From criticality to final collapse: Evolution of the *b*-value from 1.5 to 1.0. Chaos, Solitons Fractals 2009:843–53.
[37] Lozano-Ramírez NE. Finite element modeling of existing masonry towers: The Asinelli tower [Master of Science thesis]. Turin, Italy: Politecnico di Torino; 2015.